Rev. Mexicana Astron. Astrof., **13**, 137-147 (1986)

A SIMPLE, REALISTIC MODEL OF THE GALACTIC MASS DISTRIBUTION FOR ORBIT COMPUTATIONS

Christine Allen and Marco A. Martos

Instituto de Astronomía
Universidad Nacional Autónoma de México

Received 1986 July 28

RESUMEN

Se propone una función potencial $f(\tilde{\omega}, z)$ como una representación moderna y matemáticamente sencilla de la distribución de masa en nuestra galaxia. La función f es la suma de los potenciales debidos a un punto masa central, un disco elipsoidal y un halo esférico. La curva de rotación que resulta del modelo de masa es plana desde aproximadamente 17 kpc hasta 100 kpc, y representa bien los datos observados entre 1 y 17 kpc. Con un valor para la densidad local de masa de 0.18 $M_\odot$ pc^{-3} la fuerza perpendicular que resulta del modelo concuerda con la observada. El modelo implica una masa total para la galaxia de unas 10^{12} masas solares. La velocidad de escape para objetos en la vecindad solar es de 546 km s^{-1}. Los valores que se obtienen para las constantes de la rotación son A = 15.9 km s^{-1} kpc^{-1} and B = −12.2 km s^{-1} kpc^{-1}, en buena concordancia con los valores observacionales modernos. A diferencia de otros modelos recientes para la distribución de masa galáctica, el potencial que proponemos es continuo en todo sitio y tiene derivadas continuas. Su sencillez matemática lo hace especialmente apropiado para el cálculo numérico rápido y eficiente de órbitas galácticas. Como una aplicación del modelo, presentamos las órbitas galácticas de 10 estrellas cercanas de alta velocidad.

ABSTRACT

A potential function $f(\tilde{\omega}, z)$ is proposed as a modern, mathematically simple representation of the mass distribution in our galaxy. The function f is the superposition of the potential functions of a central mass point, an ellipsoidal disk and a spherical halo. The rotation curve which results from the mass model is flat from about 17 kpc out to 100 kpc, and represents well the observed values in the range 1 to 17 kpc. With an adopted value for the total local mass density of 0.18 $M_\odot$ pc^{-3} the resulting perpendicular force, K_z , also agrees well with observed values. The total galactic mass implied by the model is about 10^{12} solar masses. The escape velocity for objects in the solar vicinity is 546 km s^{-1}. The derived values for the rotation constants are A = 15.9 km s^{-1} kpc^{-1} and B = 12.2 km s^{-1} kpc^{-1}, and agree well with modern observational determinations. In contrast to other recent mass models for our galaxy, the proposed potential function is continuous everywhere, and has continuous derivatives; its simple mathematical form makes it particularly well suited for efficient and accurate numerical orbit computations. As an application, we present the results of the numerical integration of the galactic orbits of 10 nearby high velocity stars.

Key words: GALACTIC STRUCTURE – NEARBY STARS – STELLAR DYNAMICS

I. INTRODUCTION

When attempting to build a galactic mass model, it is necessary to select a few representative quantities among the many existing observational data. By varying the model parameters, one then tries to achieve a tolerably good fit to these representative points. According to the purpose for which the mass model is constructed, different sets of observational constraints will be selected.

Recent galactic mass models have concentrated in reproducing star numbers and colors for different stellar populations and in different directions, or luminosity profiles of galaxies similar to our own (Bahcall and Soneira 1980; Bahcall, Schmidt and Soneira 1983; Caldwell and Ostriker 1981, and others).

For the purpose of computing orbits we believe that a high weight should be given to those observational parameters most directly related to the forces that shape the orbit, that is, the forces in both the radial and perpendicular direction. These forces result from the global mass distribution of the galaxy. Our aim in this paper thus differs from that of other recent galactic mass models. We will develop a galactic mass model that attempts to achieve a good fit to the observational parameters directly related to the radial and perpendicular forces, while maintaining a simple mathematical form appropriate for numerical orbit computations. As a consequence, the mass components of our model will not necessarily have any direct relationship to the stellar populations. Thus, our "disk component" should not be identified with the galactic disk population, nor should our "halo component" be identified with the galactic spheroid or corona (in fact, it includes all spherically distributed matter, visible or invisible).

The paper is organized as follows: in Section II we discuss the observational constraints that the model will be required to represent, along with their uncertainties; in Section III we present the mass model; in Section IV results from the model are compared with observational data; in Section V we present, as an application, the galactic orbits of some stars of particular interest; in the final section, we give a brief summary of our results.

II. OBSERVATIONAL CONSTRAINTS

Information on $K_{\tilde{\omega}}$, the galactic force in radial ($\tilde{\omega}$) direction, is obtained from the rotation curve. The galactic rotation curve interior to the Sun has been well studied, and substantial agreement between many different determinations has been reached. As observational constraints for this part of the rotation curve we will adopt the representative points advocated by Caldwell and Ostriker (1981), which synthesize a wealth of observational data.

The rotation curve just outside the solar circle has been the subject of much controversy in recent times (Blitz 1979; Jackson, Fitzgerald and Moffat 1979; Blitz 1983). For instance, Blitz interprets the results of a study of radial motions of H II regions (Blitz, Fich and Stark 1982) as evidence for a rotation curve rising by as much as 40 km s^{-1} some 7 kpc beyond the solar circle, whereas Jackson *et al.*, obtain a more nearly flat continuation of the rotation curve. In both cases, the data are extremely noisy, and the cause of the large deviations from *any* smooth curve has not been established. A rising rotation curve beyond the Sun implies, of course, that $|B| > |A|$, which conflicts with traditional results from the kinematics of nearby stars. This disagreement is particularly worrysome, since it implies a contradiction between two sets of apparently well-determined observational data. A possible solution to this dilemma has been proposed by Haud (1984), who interprets the discrepancy as due to an oversimplification of the H II data reduction procedure. Using a comprehensive set of observational data, and taking into account non-circular motions, Haud obtains a rotation curve in good agreement with H II data inside the solar circle, gently falling just beyond the Sun, and nearly flat at larger distances.

In view of the difficulties that a rising rotation curve implies, and taking into account Haud's results, we decided to model a rotation curve that is slightly decreasing at the Sun's distance, and that remains flat at large distances. For the rotation velocity at the farthest points we adopt a value of 206 km s^{-1} (Caldwell and Ostriker 1981; Hartwick and Sargent 1978). Such a curve is typical of Sb and Sc galaxies (Rubin, Ford and Thonnard 1980). It is morphologically very similar to the rotation curve of M 31 (Roberts and Whitehurst 1975), and also to that of NGC 3200; the latter is an Sb(r)I galaxy much like our own (Rubin 1983), although the maximum value that the rotation curve reaches in this galaxy (282 km s^{-1}) is quite a bit higher than that of our adopted rotation curve; this would be consistent with a lower total luminosity for our galaxy.

Information on K_z, the perpendicular force, comes from studies of the space densities and z-motions of different groups of stars. For the purpose of comparing with observational data the run of K_z with z computed from the mass model for the solar vicinity, we use the points determined by Oort (1960) for two different values of the local density, as well as the results of Bahcall (1983) for his proportionate model with a massive halo.

The total mass density in the solar vicinity was assumed to have a value of 0.18 $M_\odot$ pc^{-3} (Bahcall 1984). In addition, we adopt R = 8 kpc as the Sun's galactocentric distance, and v = 225 km s^{-1} as the circular velocity at the Sun's position; these are reasonable compromise values among many recent determinations (Kerr and Lynden-Bell 1985; Caldwell and Ostriker 1981; Gunn, Knapp and Tremaine 1979; Knapp 1983). We will further assume that the galaxy has a total radius of 100 kpc, and we explicitly do not try to describe in detail the innermost kiloparsec.

III. THE MASS MODEL

a) *Central Mass Point*

It is well known that the mass distribution of the central region of the galaxy, as inferred from the extremely complex motions of the gas, is far from simple (Ort 1977). On the other hand, the great majority of stellar orbits of astronomical significance do not penetrate the central kiloparsec or so of the galaxy. For these orbits, even a crude approximation of the potential of the central region will be appropriate. For this reason, we will assume that the mass distribution in the central region of the galaxy is sufficiently well represented by a mass point of 0.7655×10^{10} $M_\odot$. The potential corresponding to this component is simply

$$\Phi_P = -\frac{M_c}{R} \qquad (1)$$

If R is given in kpc and M_c in galactic mass units (1 galactic mass unit = 2.32×10^7 $M_\odot$) units for Φ_P are 100 km^2 s^{-2}. We will use throughout cylindric galactic coordinates $\tilde{\omega}$, z, θ, and their corresponding velocities Π, Z, Θ. Then, $R^2 = \tilde{\omega}^2 + z^2$. The numerical constant in (1) was determined by successive trials, aiming at a good fit of the total rotation curve of the model galaxy to the observational points adopted. As expected, the innermost points of the rotation curve were most sensitive to the value of the mass of the central point, and they essentially determine it. Consistent with our assumptions, we did not try to fit closely the point at 0.4 kpc.

The central mass-point approximation we use will be quite good for orbits that do not visit the central kiloparsec or so of the galaxy. It will not be as good, but still acceptable, for very eccentric orbits, where the star spends only a short time in the central region, near pericenter. It is, of course, not intended to represent the detailed

mass distribution or the complicated dynamics near the galactic center (at $R < 0.4$ kpc), and should not be used for orbits confined to the central kiloparsec of the galaxy.

b) *Disk Component*

Recent models for the galactic mass distribution (Bahcall, Schmidt and Soneira 1983; Bahcall and Soneira 1981; Caldwell and Ostriker 1981; Rohlfs and Kreitschmann 1981) have made extensive use of exponential disks. The main motivation for this seems to be a desire to match the observed profiles for the light distribution of external spiral galaxies, which generally follow an exponential law. One disadvantage of most published models is that the potential cannot be obtained in a closed, analytical, form from the postulated density distribution. This fact seriously inhibits the numerical computation of orbits, because it makes it necessary to numerically integrate the density distribution to obtain the potential function et each point; the resulting forces have to be again numerically integrated at each point in order to arrive at the trajectory of the star. Apart from the far greater computer time necessary, an extra integration at each time step inevitably decreases the precision of the computation and –more importantly– the reliability of the orbit. A further disadvantage is that some of the published disk density distributions yield potentials that do not have continuous derivatives in the astronomically interesting regions of the galaxy (for instance, on the galactic plane) and are therefore unsuitable for orbit computations.

On the other hand, it is well known that a significant fraction, and perhaps even most, of the mass in galaxies is in the form of non-luminous matter. Even in the disks of galaxies perhaps as much as half the total mass is non-luminous matter, that may or may not follow the exponential distribution of the luminous matter. Therefore, the argument for postulating an exponential form for the distribution of *total mass* in the disk of our galaxy is not quite compelling. And, of course, it is the total mass that is relevant for orbit computations.

As we have already stated, we seek a mathematically simple representation of the galactic potential, which will yield satisfactory agreement with those observed parameters that are most sensitive to the overall, total, mass distribution in our galaxy, namely, the rotation curve and the perpendicular force. In other words, we have no reason to prefer an exponential to an ellipsoidal disk as long as the latter gives satisfactory agreement with the rotation curve and the perpendicular force. In fact, if the latter can be expressed in a simple, closed, form, it will be preferable for our purpose. For these reasons, we decided to abandon an exponential representation for the mass distribution of the disk, and to experiment with a modified ellipsoidal distribution.

For the potential of an ellipsoidal Schmidt-type galaxy (Schmidt 1956) a mathematically simple interpolation formula was developed and carefully tested by Ollongren (1962). This formula was very successful; indeed, it was used for nearly all the computations of orbits in galactic-type potentials that were carried out for many years after its publication. Its use was gradually abandoned as it became increasingly clear that the rotation curve of our galaxy remains essentially flat to distances of 50 or more kpc, and that therefore a Schmidt-type potential is not a satisfactory representation of its mass distribution.

For the potential function of the galactic disk in our model we use a modification of Ollongren's interpolation formula that consists essentially in a rescaling of the disk component to conform, when added to the other components, with the adopted rotation curve. Specifically, we assume that the potential due to the disk is represented by

$$\Phi_D(\tilde{\omega}, z) = A\,\Phi_{IF}(B\tilde{\omega}, Cz);$$
$$\Phi_{IF}(\tilde{\omega}, z) = -1000/\sqrt[4]{Q_{IF}}\,, \tag{2}$$

where

$$Q_{IF}(\tilde{\omega}, z) = P_n + \frac{P_a}{P_b} - \frac{P_c}{P_k} + \frac{P_c}{P_k + z^2} + P_m. \tag{3}$$

is Ollongren's (1962) interpolation formula, and the polynomials are

$$P_n = n_4\tilde{\omega}^4 + n_2\tilde{\omega}^2 + n_0\,,$$
$$P_a = a_8\tilde{\omega}^8\,,$$
$$P_b = \tilde{\omega}^4 + b_2\tilde{\omega}^2 + b_0\,,$$
$$P_c = c_6\tilde{\omega}^6 + c_4\tilde{\omega}^4 + c_0\,, \tag{4}$$
$$P_k = k_{10}\tilde{\omega}^{10} + k_2\tilde{\omega}^2 + k_0\,,$$
$$P_m = m_4 z^4 + 2m_4\tilde{\omega}^2 z^2 + m_2 z^2\,;$$

For easy reference, we list in Table 1 the constants that enter into Ollongren's formula. Units for Φ_D are again 100 km^2 s^{-2}, if $\tilde{\omega}$ and z are given in kpc. The constant A determines the relative importance of the disk component, and was obtained from the fit of the total rotation curve to the adopted observational constraints. The inner part of the rotation curve is most sensitive to A. B is a scaling constant, and C was adjusted to fix the local mass density at a value of 0.18 $M_\odot$ pc^{-3}.

TABLE 1

CONSTANTS FOR DISK

n_0 =	0.34178	c_4 =	$-0.6607 \cdot 10^{-3}$
n_2 =	0.14023	c_6 =	$-0.9516 \cdot 10^{-5}$
n_4 =	$0.1184 \cdot 10^{-2}$	k_0 =	0.2
a_8 =	$0.139 \cdot 10^{-1}$	k_2 =	$0.1045 \cdot 10^{-1}$
b_0 =	$4.21937 \cdot 10^{3}$	k_{10} =	$0.12464 \cdot 10^{-10}$
b_2 =	$0.7857 \cdot 10^{2}$	m_2 =	0.59
c_0 =	$-0.4 \cdot 10^{-1}$	m_4 =	$0.14084\ 10^{-1}$

c) *Halo Component*

In order to flatten the rotation curve at large galactocentric distances several forms of massive haloes have been proposed in the literature (Knapp 1983; Bahcall, Schmidt and Soneira 1983; Bahcall and Soneira 1981; Caldwell and Ostriker 1981; Rohlfs and Kreitschmann 1981). It has even been suggested that a fairly flat rotation curve (at least out to about 30 kpc) can be obtained without invoking a massive halo (Shuter 1981; Schmidt 1983). This idea has not been generally accepted however, because it implies very special mass distributions for the disk and spheroidal components, in contradiction with observational data.

In our model, the mass distribution of the halo has the form

$$M(R) = \frac{\alpha (R/\beta)^{\gamma}}{1 + (R/\beta)^{\gamma-1}} , \qquad (5)$$

which, of course, has the desired asymptotic dependence $M(R) \sim R$ for large values of R. If R is given in kpc, the resulting units for M are galactic mass units. The constant α is analogous to A when R is not large, and it was similarly determined. β was assumed to have a value of 10 kpc. The exponent γ was adjusted until a good fit to the observed rotation curve was obtained. The outer part of the rotation curve, especially the point at 53 kpc, turned out to be very sensitive to the exponent. The total mass of the halo out to 100 kpc is $9.4 \times 10^{11}\ M_{\odot}$. The halo contributes $0.009\ M_{\odot}\,pc^{-3}$ to the local mass density.

The potential implied by the halo mass distribution (5) is

$$\Phi_H(R) = -\frac{M(R)}{R} - \int_R^{100} \frac{1}{R'} \frac{dM(R')}{dR'} dR' . \qquad (6)$$

Units for Φ_H are 100 $km^2\ s^{-2}$ if R is given in kpc and M(R) in galactic mass units. Equation (6) includes an arbitrary cutoff for the halo at 100 kpc. For computations involving orbits that reach apogalactic distances larger than 100 kpc a correspondingly larger halo cutoff can easily be incorporated in the mass model. Note that although the halo potential given by (6) cannot be expressed in closed form, its derivatives (the forces) can indeed be analytically calculated at each point of the trajectory. Thus, the integral that appears in (6) is of no import for orbit computations. When numerically integrating a trajectory, it is only necessary to evaluate that integral at conveniently long intervals in order to compute the total energy of the orbiting particle at that time, and to check how accurately it is conserved.

The total potential is then

$$\Phi = \Phi_P + \Phi_D + \Phi_H . \qquad (7)$$

IV. COMPARISON OF THE MASS MODEL WITH OBSERVATIONAL DATA

Table 2 summarizes the assumed observational constraints and the constants used for the fit of our mass model. In Table 3 are listed the contributions to the rotation curve arising from the three mass components of the model, and the total rotation curve. Figure 1 shows the rotation curve of each of the three components, and Figure 2 the total rotation curve together with the observational data adopted by Caldwell and Ostriker (1981) for points interior to the solar circle, as well as three exterior points: at R = 10 kpc and R = 15 kpc (scaled and averaged from Haud's (1984) values) and at R = 53 kpc (Caldwell and Ostriker 1981, computed and scaled from Hartwick and Sargent 1978). The error bars represent the estimated urcertainties in the data. It can be easily seen that the overall agreement is very good.

TABLE 2

ADOPTED OBSERVATIONAL CONSTRAINTS AND CONSTANTS

Distance Sun – Galactic Center:	$\tilde{\omega}_0$ = 8 kpc	
Local circular Velocity:	Θ_0 = 225 km s^{-1}	
Local total mass density:	ρ_0 = 0.18 $M_{\odot}\,pc^{-3}$	
Rotation curve:	$\tilde{\omega}$ (kpc)	Θ (km s^{-1})
	0.4	260 ± 10
	1.2	227 ± 10
	2.4	203 ± 10
	4.0	216 ± 10
	6.0	228 ± 10
	10.0	209 ± 15
	15.0	223 ± 20
	53.3	206 ± 40
Point mass constant:	$M_C = 7.656 \times 10^9\ M_{\odot}$	
Disk constants:	C = 1.742, A = 0.574, B = 1.025	
Halo constants:	β = 10 kpc	
	α = 4442.024	
	γ = 2.02	

TABLE 3

CONTRIBUTIONS TO THE ROTATION CURVE

$\tilde{\omega}$ (kpc)	Θ (km s^{-1})	Mass Point (km s^{-1})	Disk (km s^{-1})	Halo (km s^{-1})
1	217.66	181.66	102.48	62.23
2	207.57	128.45	139.21	84.89
3	208.53	104.88	149.74	100.31
4	213.47	90.83	157.46	111.92
5	221.19	81.24	166.30	121.12
6	226.83	74.16	171.47	128.65
7	227.70	68.66	170.06	134.96
8	224.99	64.23	163.71	140.33
9	220.83	60.55	155.18	144.98
10	216.61	57.45	146.32	149.03
15	204.15	46.90	112.86	163.52
20	200.77	40.62	94.38	172.48
25	200.20	36.33	82.87	178.59
30	200.50	33.17	74.86	183.02
35	201.06	30.71	68.86	186.39
40	201.67	28.72	64.14	189.03
45	202.26	27.08	60.30	191.16
50	202.81	25.69	57.08	192.91
60	203.76	23.45	51.97	195.62
70	204.53	21.71	48.03	197.62
80	205.16	20.31	44.88	199.16
90	205.68	19.15	42.28	200.38
100	206.12	18.17	40.09	201.37

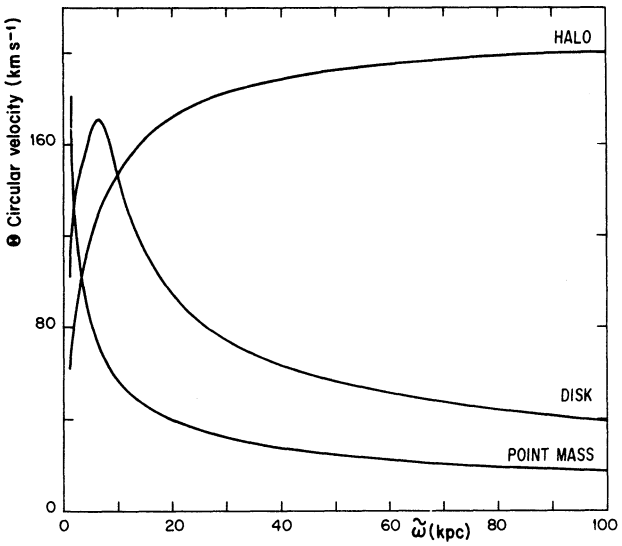

Fig. 1. Contributions of the three mass components to the rotation cure.

Table 4 lists the perpendicular force, K_z, as a function of z for $\tilde{\omega} = 8$ kpc. Figure 3 shows this force along with the data obtained by Oort (1960, 1965), for two values of the local density, 0.18 and 0.15 $M_\odot$ pc^{-3} (his preferred value); also shown are the values obtained by Bahcall (1984) for a galactic model in which the unobserved matter is distributed like the observed matter, and which includes a massive halo. We can see that the observational determinations are in essential agreement only for small values of z. For z larger than about 100 pc the Bahcall data are always lower than the Oort results for both plot-

TABLE 4

RUN OF K_z VERSUS z FOR $\tilde{\omega}$ = 8 kpc

z (pc)	$-K_z$ (10^{-9} cm s^{-2})	z (pc)	$-K_z$ (10^{-9} cm s^{-2})
100	2.96	1200	8.31
200	5.14	1300	8.55
300	6.35	1400	8.77
400	6.86	1500	8.98
500	7.04	2000	9.70
600	7.13	2500	9.96
700	7.24	3000	9.91
800	7.39	3500	9.69
900	7.59	4000	9.38
1000	7.82	4500	9.03
1100	8.06	5000	8.65

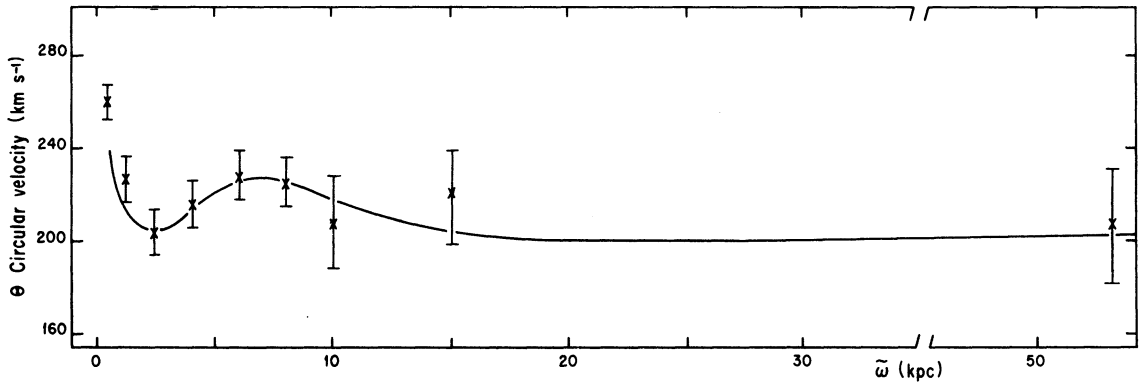

Fig. 2. Total rotation curve resulting from the mass model. The error bars are the estimated uncertainties in the observational data.

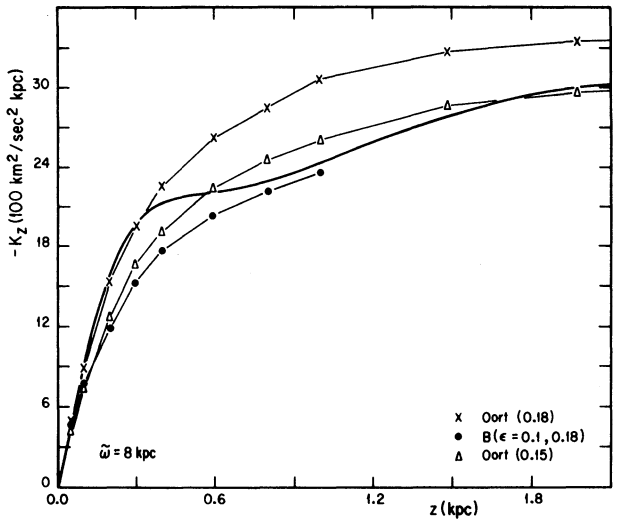

Fig. 3. The perpendicular force K_Z as a function of z (solid line). The points shown are the data of Oort (1960) for two values of the local density, $\rho = 0.15\ M_\odot\ pc^{-3}$ (triangles) and $\rho = 0.18\ M_\odot\ pc^{-3}$ (crosses). Also shown are the values obtained by Bahcall (1984) for his proportionate model with a massive halo (dots).

ted values of the local density; in fact, they resemble most the results obtained by Oort for the lowest density value he considered (not plotted), namely, $0.12\ M_\odot\ pc^{-3}$. The perpendicular force resulting from our model increases steeply at first, closely following Oort's data for $\rho = 0.18\ M_\odot\ pc^{-3}$ out to about 300 pc; it then becomes flatter, and begins to resemble the data of Bahcall. At z = 1000 pc it is in substantial agreement with the latter. At still larger z, our model results are similar to Oort's data for a value $\rho = 0.15\ M_\odot\ pc^{-3}$. In view of the considerable uncertainty of the observational determinations, the results obtained from the mass model can be considered to be a satisfactory representation of the data.

Figure 4 shows the run of K_z with z for different values of $\tilde{\omega}$. Note that in the solar vicinity K_z reaches a maximum value of $-K_z = 9.9 \times 10^{-9}$ cm s^{-2} at z = 3.3 kpc which is similar to the observational value $-K_z = 9.1 \times 10^{-9}$ cm s^{-2} (Caldwell and Ostriker 1981).

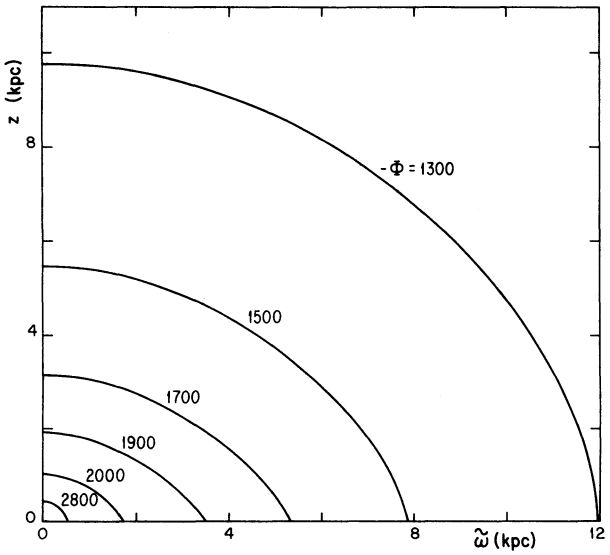

Fig. 5. Some equipotential surfaces resulting from the mass model, shown in the plane $\tilde{\omega}$, z.

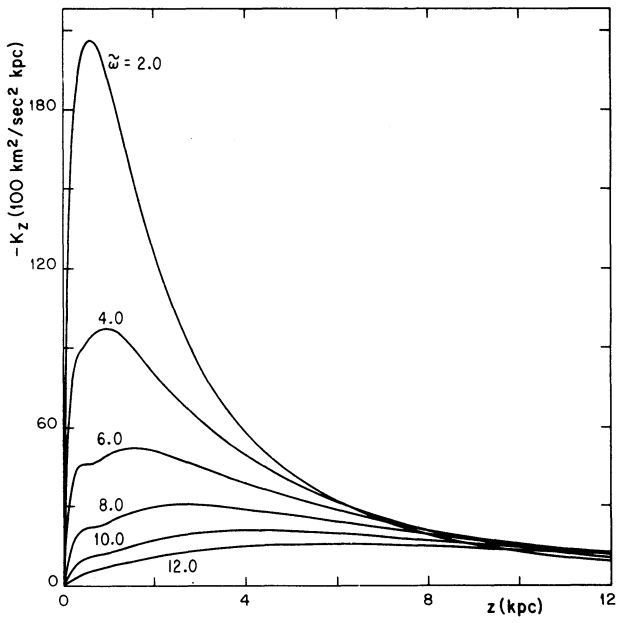

Fig. 4. Run of K_Z as a function of z for different values of $\tilde{\omega}$.

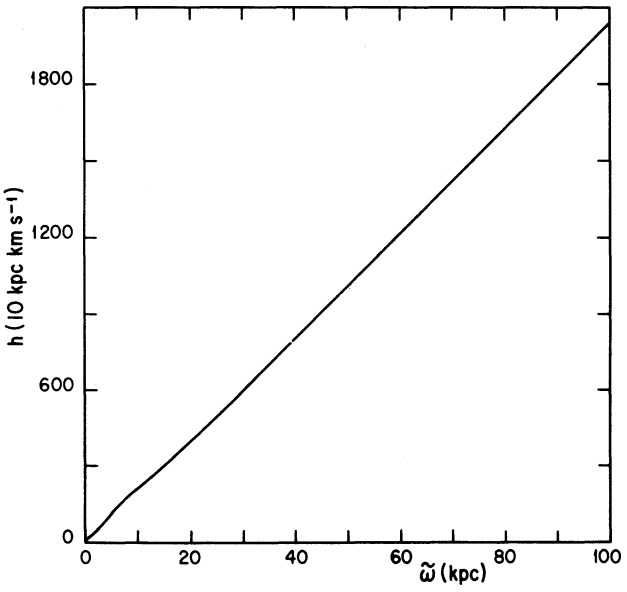

Fig. 6. The orbital angular momentum h as a function of $\tilde{\omega}$ for circular orbits. The diagram shows that all circular orbits are stable, since h always increases with $\tilde{\omega}$.

Figure 5 shows a few equipotential surfaces; it is seen that they are smooth everywhere, and nearly spherical already at moderate distances from the plane. The stability of all plane circular orbits in our potential is demonstrated in Figure 6, where it is shown that h, the orbital angular momentum, increases with $\tilde{\omega}$ everywhere (Chandrasekhar 1942).

Table 5 lists some local parameters computed from our mass model. The derived values for Oort's constants are A = 15.9 km s^{-1} kpc^{-1} and B = −12.2 km s^{-1} kpc^{-1}, well within the range of currently accepted observational values (Kerr and Lynden-Bell 1985; Caldwell and Ostriker 1981; Gunn; Knapp and Tremaine 1979; Knapp 1983). The local centroid moves with an angular velocity θ of 28.1 km s^{-1} kpc^{-1} and the local slope of $\Theta(\tilde{\omega})$ is −3.7 km s^{-1} kpc^{-1}, corresponding to a gently falling rotation curve at the solar position.

The escape velocity in the solar vicinity is v_e = 545.9 km s^{-1}. Values for $v_e > 550$ km s^{-1} are typical of galactic mass models that include a massive halo. Currently accepted values for v_e fall in the range $v_e = 640 \pm 96$ km s^{-1} (Caldwell and Ostriker 1981). Table 6 lists the escape velocity for different values of $\tilde{\omega}$.

TABLE 5

LOCAL PARAMETERS COMPUTED FROM THE MODEL

Rotation constant	A =	15.9 km s^{-1} kpc^{-1}
Rotation constant	B =	−12.2 km s^{-1} kpc^{-1}
Period of revolution of local centroid	P =	2.15×10^8 y
Angular velocity of local centroid	$\dot{\theta}_0$ =	28.1 km s^{-1} kpc^{-1}
Local slope of Θ	$\left[\frac{d\Theta}{d\tilde{\omega}}\right]_{\tilde{\omega}_0}$ =	−3.7 km s^{-1} kpc^{-1}
Escape velocity	v_e =	545.9 km s^{-1}
Density gradient	$\tilde{\omega}_0 \frac{d}{d\tilde{\omega}}(\log \rho)$ =	−1.43

TABLE 6

ESCAPE VELOCITY AS A FUNCTION OF $\tilde{\omega}$

$\tilde{\omega}$ (kpc)	v_e (km s^{-1})	$\tilde{\omega}$ (kpc)	v_e (km s^{-1})
1	699.3	20	465.9
2	653.9	25	446.2
3	626.5	30	429.5
4	605.8	35	414.8
5	588.3	40	401.5
6	572.4	45	389.4
7	558.3	50	378.1
8	545.9	60	357.6
9	535.0	70	339.2
10	525.5	80	322.2
15	490.4	90	306.4
		100	291.5

V. ORBITS OF NEARBY, HIGH VELOCITY, STARS

As an application, we computed the galactic orbits of 10 nearby high-velocity stars. These stars were selected from van de Kamp's (1971) list of stars nearer than 5.2 pc. The reasons for selecting nearby stars of high velocity are (a) that for these stars sufficient observational material exists for determining their present positions and velocities with respect to the galactic center (which serve as "initial conditions" for the integration of the orbit), and (b) that the usual epicycle approximation is not very good for these stars, since their motions presumably deviate strongly from planar circular motions. In addition, these stars, being situated as they are in the immediate solar neighborhood, are interesting in their own right.

The orbits of the stars were numerically integrated

TABLE 7

OBSERVED PARAMETERS AND INITIAL CONDITIONS FOR NEARBY STARS (r < 5.2 pc)

G1	α (h m s)	δ (° ′)	π (″)	V_r (km s^{-1})	$\mu_\alpha \cos\delta$ (″ y^{-1})	μ_δ (″ y^{-1})	U	V	W (km s^{-1})	$\tilde{\omega}$ (kpc)	z (kpc)	Π	Z	Θ (km s^{-1})
1	00 02 28	−37 36.2	.225	23	5.648	−2.329	− 77	− 99	−35	7.999	−0.004	+ 68.2	−28.5	+137.7
166	04 12 58	−07 43.8	.205	− 42	−2.231	−3.420	95	− 12	−40	8.004	−0.003	−103.7	−32.8	+225.4
191	05 09 41	−44 59.9	.256	245	6.595	−5.702	19	−288	−52	8.001	−0.002	− 28.2	−45.5	− 51.0
411	11 00 37	36 18.3	.397	− 84	−0.566	−4.743	46	− 53	−74	8.001	0.002	− 54.8	−66.6	184.1
445	11 44 35	78 57.7	.196	−119	0.750	0.480	71	− 60	−77	8.002	0.003	− 79.9	−70.4	+177.1
699	17 55 23	04 33.3	.552	−108	−0.750	10.310	−138	6	19	7.998	0.000	+129.4	+25.6	+242.5
820	21 04 40	38 30.0	.296	− 64	4.136	3.185	− 90	− 53	− 8	8.000	0.000	+ 81.3	− 1.2	+183.5
845	21 59 33	−56 59.6	.291	− 40	3.940	−2.555	− 77	− 38	4	7.998	−0.003	+ 68.3	+10.8	+199.0
887	23 02 39	−36 8.5	.279	10	6.776	1.310	−102	− 15	−57	7.999	−0.003	+ 92.8	−50.0	+222.3
905	23 39 26	43 55.2	.318	− 81	0.110	−1.600	34	− 77	1	8.001	−0.001	− 42.5	+ 8.2	+159.5

back wards in time for 1.2×10^{10} years, an estimated upper limit to the ages of the old nearby stars. The integrating routine used incorporates a seventh order Runge-Kutta-Fehlberg algorithm with automatic step control (Fehlberg 1968). Typically, we had errors in the total energy and in the z-component of the angular momentum of the star of, respectively, $\Delta E/E < 10^{-6}$ and $\Delta h/h < 10^{-8}$ at the end of the run. The computing time for each orbit was about 5 minutes on a Prime 550 computer. The accuracy and the speed of the runs demonstrate the suitability of our model mass distribution for direct numerical integrations of galactic orbits.

Table 7 lists the observed parameters and the derived "initial conditions" for the selected stars, Table 8 the main characteristics of their galactic orbits.

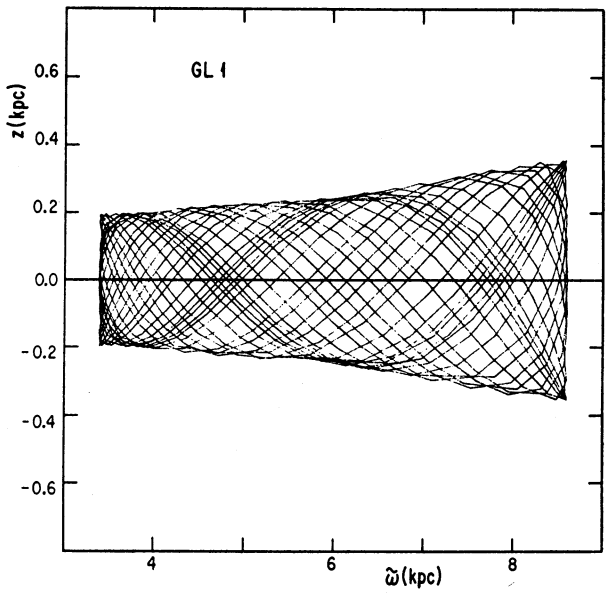

Fig. 7. The meridional orbit of Gliese 1.

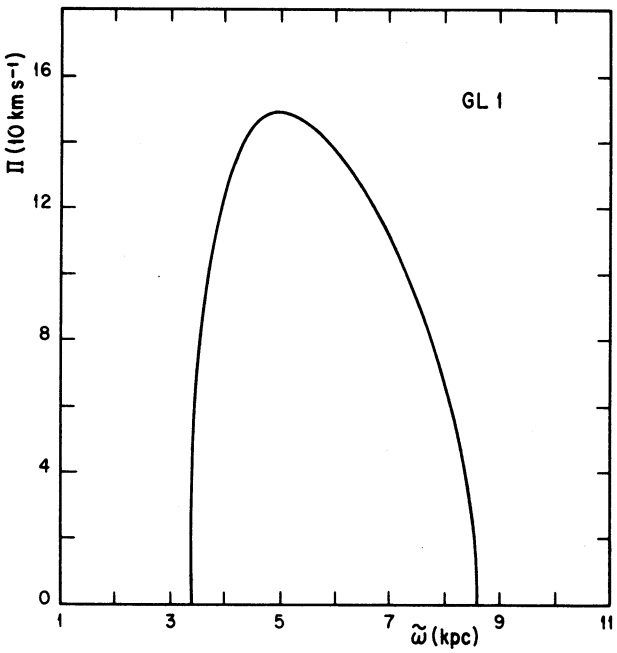

Fig. 8. The surface of section for the orbit of Gliese 1.

The computed orbits do indeed strongly deviate from circular orbits. Their galactic periods of revolution are all between 1.3 and 2.3 Gy, somewhat longer than expected for nearby stars. This is due to the high "eccentricity" of their orbits: most of them show radial excursions of over 4 kpc. G1 411 and G1 445, the least "eccentric" orbits, still have radial excursions of over 3 kpc. G1 191 (Kapteyn's star) is the orbit of highest "eccentricity"; also, it is retrograde. G1 699 (Barnard's star) reaches the largest apogalactic distance, and G1 445 the largest height above and below the galactic plane. The "eccentricities" of the computed orbits would be consistent with those of halo stars. However, none of the orbits reach extreme values

TABLE 8

PRINCIPAL CHARACTERISTICS OF GALACTIC ORBITS OF NEARBY STARS

G1	Energy E (100 km^2 s^{-2})	Angular momentum h (10 km kpc s^{-1})	$\tilde{\omega}_{min}$ (kpc)	$\tilde{\omega}_{max}$ (kpc)	z_{min} (kpc)	z_{max} (kpc)	⟨Period⟩ (10^8 years)	"Eccentricity" $\left(\frac{\tilde{\omega}_{max} - \tilde{\omega}_{min}}{\tilde{\omega}_{max} + \tilde{\omega}_{min}}\right)$
1	−1367.77	110.15	3.38	8.61	−0.36	0.36	1.33	0.44
166	−1176.41	180.41	5.98	12.39	−0.55	0.55	1.88	0.35
191	−1462.42	−40.82	0.94	8.07	−0.65	0.65	1.37	0.79
411	−1283.07	147.31	5.51	8.85	−1.27	1.27	1.69	0.23
445	−1276.13	141.71	4.99	9.54	−1.50	1.50	1.47	0.31
699	−1108.79	193.99	5.95	15.60	−0.48	0.48	2.29	0.45
820	−1288.47	146.77	4.87	9.39	−0.01	0.01	1.43	0.32
845	−1268.03	159.16	5.59	9.32	−0.13	0.13	2.09	0.25
887	−1187.30	177.79	6.12	11.81	−1.09	1.09	2.08	0.32
905	−1353.17	127.62	4.23	8.29	−0.09	0.09	1.50	0.32

of z. The highest orbit, that of G1 445 reaches a z-distance of 1.5 kpc. On the basis of their z-motions, this group of stars would belong to an old, thick disk population. Their observed spectra and colors would, on the whole, be consistent with this classification.

Figures 7, 9 to 13, and 15 to 18 show the meridional orbits of the stars. Figure 8 shows a typical surface of section, which corresponds to the orbit of G1 1; all orbits except that of G1 166 (40 Eridani) and G1 699 (Barnard's star) are box-orbits, and have surfaces of section similar to that of Figure 8. Figure 14 shows the surface of section of the orbit of G1 699. We see that this star moves around the galaxy in a shell-type orbit, and that there are regions of the radial axis interior to the orbit that are never visited by the star. The orbit of the triple system G1 166 is of similar form.

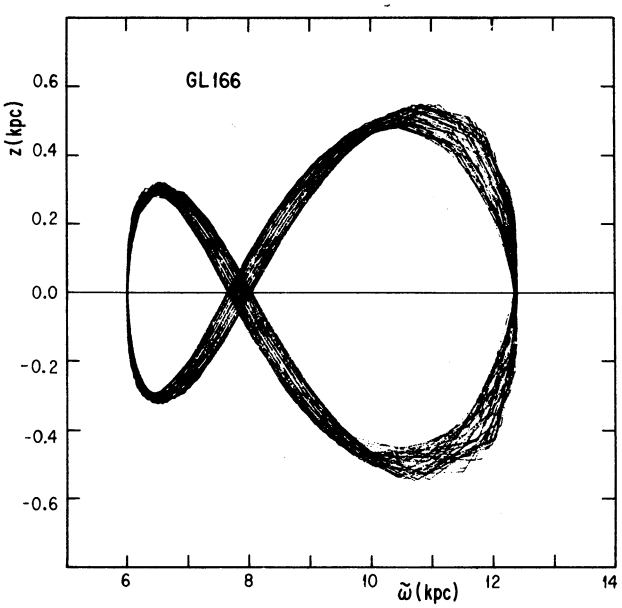

Fig. 9. The meridional orbit of Gliese 166.

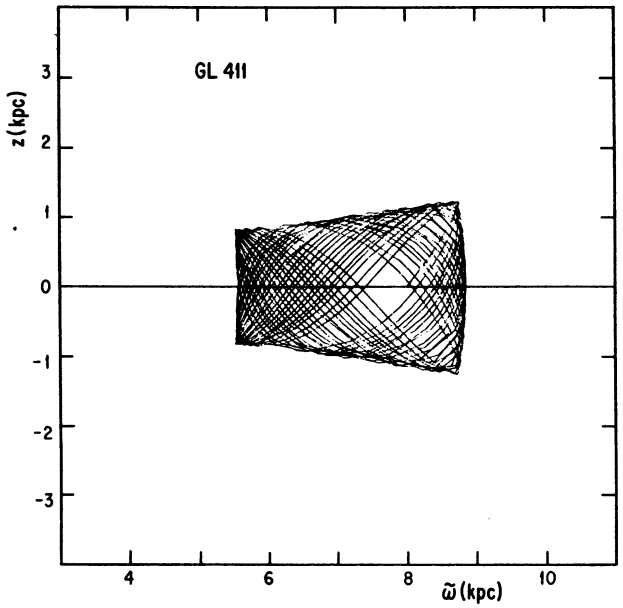

Fig. 11. The meridional orbit of Gliese 411.

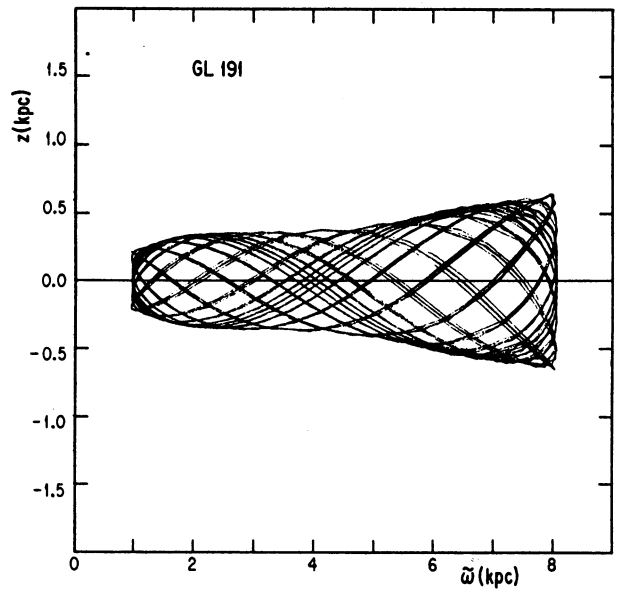

Fig. 10. The meridional orbit of Gliese 191.

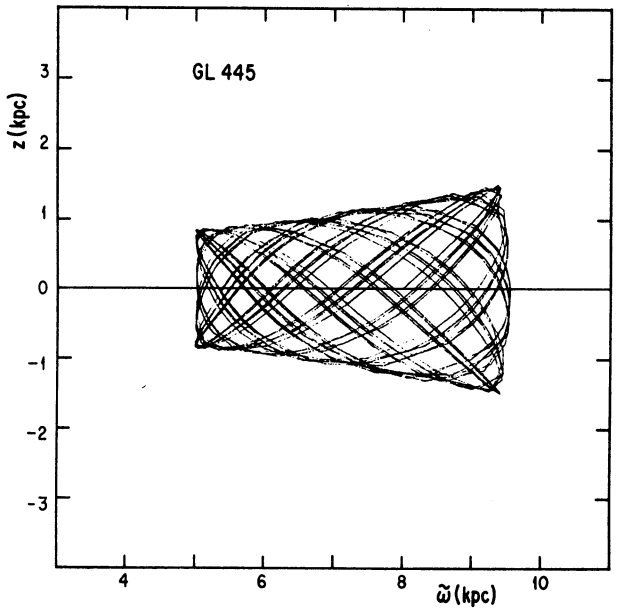

Fig. 12. The meridional orbit of Gliese 445.

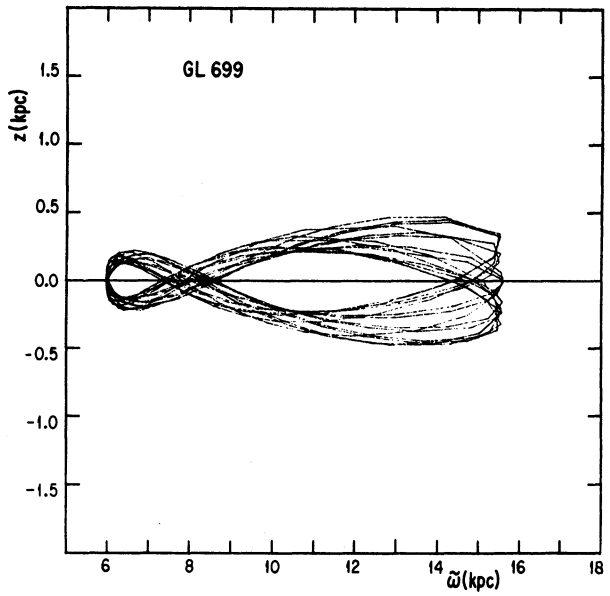

Fig. 13. The meridional orbit of Gliese 699.

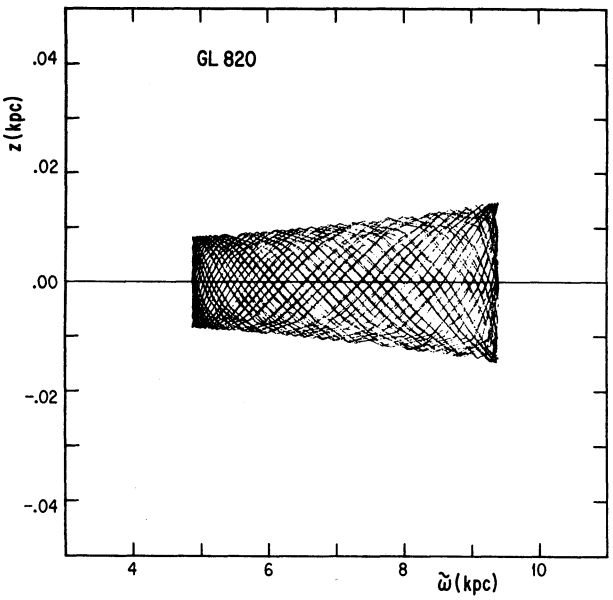

Fig. 15. The meridional orbit of Gliese 820.

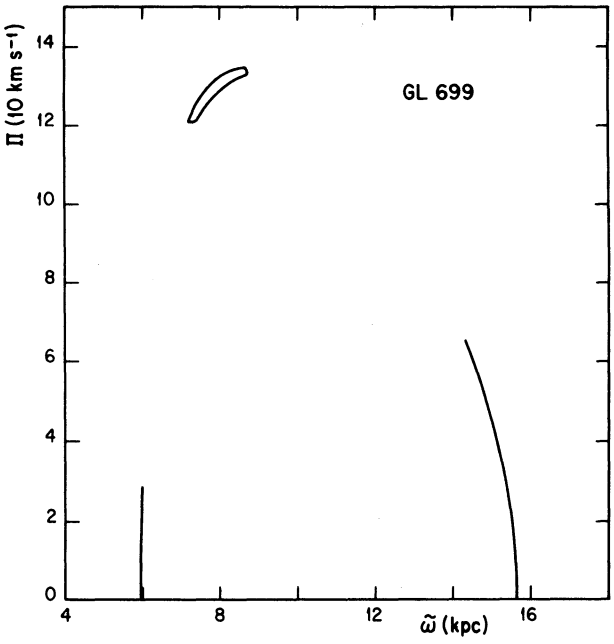

Fig. 14. The surface of section for the orbit of Gliese 699.

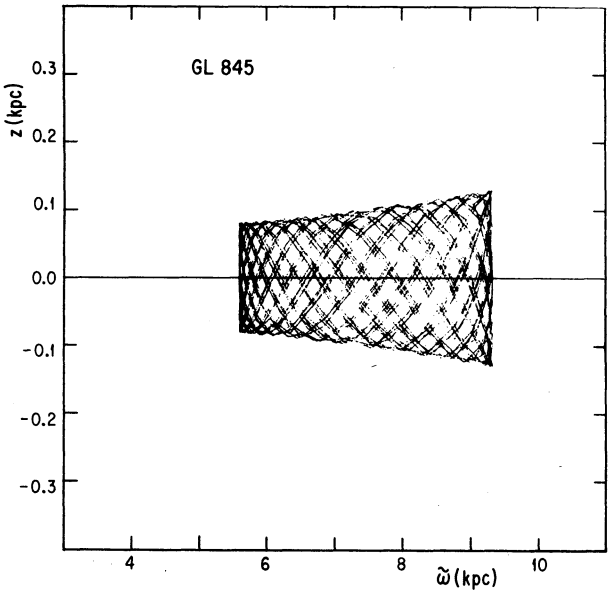

Fig. 16. The meridional orbit of Gliese 845.

VI. CONCLUSIONS AND SUMMARY

A mathematically simple model for the mass distribution of the galaxy has been presented. It was shown that the model represents well the rotation curve and the perpendicular force of the galaxy. The rotation constants implied by the model are within the range of currently accepted values.

As an illustration, the galactic orbits of a group of 10

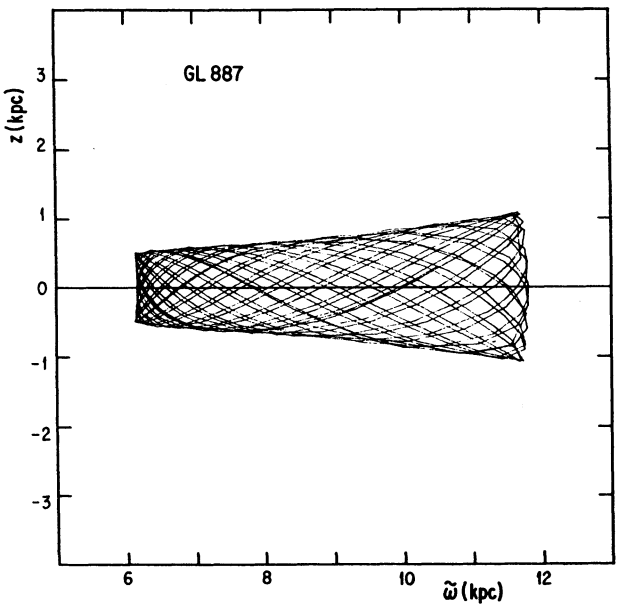

Fig. 17. The meridional orbit of Gliese 887.

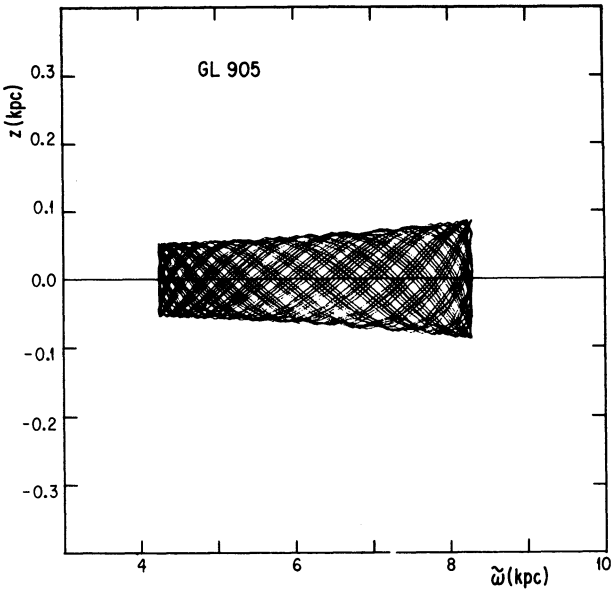

Fig. 18. The meridional orbit of Gliese 905.

nearby high velocity stars were numerically integrated. The speed with which the integrations were carried out, as well as the high accuracy of the conservation of the energy and angular momentum, show that the mass model indeed allows efficient and accurate numerical orbit computations.

The computed orbits show very large excursions in the radial coordinate but they reach, in general, only moderately high distances from the galactic plane. Thus, they cannot be identified as extreme halo objects, but rather as belonging to an old, thick disk population.

We would like to express our gratitude to A. Poveda, E. Moreno and J.M. Rodríguez-Espinoza for fruitful discussions. Part of this work was done while C.A. was on sabbatical leave, and thanks are due to the Center for Astrophysics and Space Science of the University of California at La Jolla for their warm hospitality, and to Conacyt for financial assistance. Some of the computations were performed at Ensenada, and we thank CICESE for the use of their computer, as well as for friendly assistance.

REFERENCES

Bahcall, J.N. 1984, *Ap. J.*, **276**, 169.
Bahcall, J.N. and Soneira, R.M. 1981, *Ap. J. Suppl.*, **47**, 357.
Bahcall, J.N., Schmidt, M. and Soneira, R. 1982, *Ap. J. (Letters)*, **258**, L23.
Bahcall, J.N., Schmidt, M. and Soneira, R. 1983, *Ap. J.*, **265**, 730.
Blitz, L. 1983, in *Kinematics, Dinamics and Structure of the Milky Way*, ed. W.L.H. Shuter (Dordrecht: D. Reidel), p. 143.
Blitz, L., Fich, M., and Stark, A.A. 1982, *Ap. J. Suppl.*, **49**, 183.
Caldwell, J.A.R., and Ostriker, J.P. 1981, *Ap. J.*, **251**, 61.
Chandrasekhar, S. 1942, in *Principles of Stellar Dynamics* (Chicago: U. of Chicago Press), p. 155.
Fehlberg, E. 1968, *NASA TR R-287.*
Gunn, J.E., Knapp G.R. and Tremaine, S.D. 1979, *A. J.*, **84**, 1181.
Hartwick, F.D.A. and Sargent, W.L.W. 1978, *Ap. J.*, **221**, 512.
Haud, U. 1984, *Ap. Space Scie.*, **104**, 337.
Jackson, P.D., Fitzgerald, M.P. and Moffat, A.F.J. 1979, in *IAU Symposium 84, The Large-Scale Characteristics of the Galaxy*, ed. W.R. Burton, (Dordrecht: D. Reidel), p. 221.
Kerr, F.J. and Lynden-Bell, D. 1985, *Report to IAU Comm. 33.*
Knapp, G.R. 1983, in *Kinematics, Dynamics and Structure of the Milky Way*, ed. W.L.H. Shuter (Dordrecht: D. Reidel), p. 233.
Ollongren, A. 1962, *Bull. Astr. Inst. Netherlands*, **16**, 241.
Oort, J.H. 1960, *Bull. Astr. Inst. Netherlands*, **15**, 45.
Oort, J.H. 1965, in "Galactic Structure", ed. A. Blaauw and M. Schmidt (Chicago: The University of Chicago Press), p. 455.
Oort, J.H. 1977, *Ann. Rev. Astr. Ap.*, **15**, 295.
Roberts, M.S. and Whitehurst, R.N. 1975, *A. J.*, **201**, 327.
Rohlfs, K. and Kreitschmann, J. 1981, *Ap. Space Scie.*, **79**, 289.
Rubin, V.C. 1983, in *Kinematics, Dynamics and Structure of the* Milky Way, ed. W.L.H. Shuter (Dordrecht: D. Reidel), p. 379.
Rubin, V.C., Ford, W.K., and Thonnard, N. 1980, *Ap. J.*, **238**, 471.
Schmidt, M. 1956, *Bull. Astr. Inst. Netherlands*, **13**, 15.
Shuter, W.L. 1981, *M.N.R.A.S.*, **194**, 851.
van de Kamp, P. 1971, *Ann. Rev. Astr. Ap.*, **9**, 103.

Christine Allen and Marco A. Martos: Instituto de Astronomía, UNAM, Apartado Postal 70-264, 04510 México, D.F., México.